Aberrant epithelial morphology and persistent epidermal growth factor receptor signaling in a mouse model of renal carcinoma

Zachary S. Morris and Andrea I. McClatchey[1]

Massachusetts General Hospital Center for Cancer Research and Department of Pathology, Harvard Medical School, Charlestown, MA 02129

Edited by Robert A. Weinberg, Whitehead Institute for Biomedical Research, Cambridge, MA, and approved April 24, 2009 (received for review February 24, 2009)

The epidermal growth factor receptor (EGFR) has frequently been implicated in hyperproliferative diseases of renal tubule epithelia. We have shown that the NF2 tumor suppressor Merlin inhibits EGFR internalization and signaling in a cell contact–dependent manner. Interestingly, despite the paucity of recurring mutations in human renal cell carcinoma (RCC), homozygous mutation of the *NF2* gene is found in ≈2% of RCC patient samples in the Sanger COSMIC database. To examine the roles of Merlin and EGFR in kidney tumorigenesis, we generated mice with a targeted deletion of *Nf2* in the proximal convoluted epithelium using a *Villin-Cre* transgene. All of these mice developed intratubular neoplasia by 3 months, which progressed to invasive carcinoma by 6–10 months. Kidneys from these mice demonstrated marked hyperproliferation and a concomitant increase in label-retaining putative progenitor cells. Early lumen-filling lesions in this model exhibited hyperactivation of EGFR signaling, altered solubility of adherens junctions components, and loss of epithelial polarity. Renal cortical epithelial cells derived from either early or late lesions were dependent on EGF for in vitro proliferation and were arrested by pharmacologic inhibition of EGFR or re-expression of *Nf2*. These cells formed malignant tumors upon s.c. injection into immunocompromised mice before in vitro passage. Treatment of *Vil-Cre;Nf2*$^{lox/lox}$ mice with the EGFR inhibitor erlotinib halted the proliferation of tumor cells. These studies give added credence to the role of EGFR signaling and perhaps *Nf2* deficiency in RCC and describe a rare and valuable mouse model for exploring the molecular basis of this disease.

EGFR | kidney | Merlin | Nf2 | renal cell carcinoma

Renal cell carcinomas (RCC) arise from renal tubule epithelial cells and account for 85% of kidney tumors (1). Most cases of RCC are sporadic (>97%), yet hereditary syndromes, such as Von Hippel-Lindau, hereditary papillary renal carcinoma, Birt-Hogg-Dubé, hereditary leiomyomatosis and renal cell cancer, and tuberous sclerosis complex, contribute to disease incidence (2). Somatic mutations in the genes associated with these syndromes—*VHL*, c-*Met*, *BHD*, *FH, TSC-1*, and *TSC-2*, respectively—have been identified in sporadic RCC (3, 4). Studies of the cellular consequences of specific genetic mutations associated with hereditary RCCs have spawned much of our current understanding of tumorigenesis from renal tubule epithelia. Yet these well-studied genetic events do not account for the totality of sporadic tumorigenesis in RCC, suggesting that additional causative mutations remain unidentified (5).

Studies of RCC pathogenesis have been limited by the paucity of genetically defined animal models. Surprisingly, mice with genetic disruptions of *VHL*, *c-Met*, or *FH* do not develop kidney tumors (6–8). To date, only mutation of *BHD*, *TSC-1*, *TSC-2*, or the *APC* tumor suppressor yields tumors reminiscent of RCC in genetically engineered animals (9–14). Yet mutation of these genes is rare in sporadic RCC, and these animal models provide an incomplete picture of the diverse molecular mechanisms implicated in this disease. Moreover, none of these models is ideal for studying renal tumorigenesis, owing to high neonatal mortality (*BHD*, *APC*), long latency of tumor development (*TSC-1*), or lack of tissue-specific targeting (*TSC-1*, *TSC-2*) (9–14). Additional and improved animal models of RCC are needed to advance basic and preclinical studies of renal epithelial neoplasia.

The paucity of recurrent genetic alterations that have been identified in RCC is striking. According to the Sanger Catalog of Somatic Mutations in Cancer (COSMIC) database (15), only 3 genes are mutated at a frequency greater than 4% in RCC patient samples (*VHL*, 42%; *CDKN2A*, 12%; and *KIT*, 8%). The fact that homozygous mutation of the *neurofibromatosis type 2* (*NF2*) tumor suppressor gene was identified in ≈2% (2 of 126) of the RCC samples in this database is therefore potentially significant, especially in light of the associations between aberrant epidermal growth factor receptor (EGFR) signaling and both RCC and *Nf2* (16–20). We recently demonstrated that the *Nf2* tumor suppressor Merlin is a critical regulator of EGFR (17, 21). In a variety of cellular contexts Merlin coordinates the inhibition of EGFR signaling with the establishment of stable adherens junctions (AJs) (22), thereby mediating contact-dependent inhibition of proliferation. It is well documented that EGFR and its ligands, EGF and TGF-α, are frequently overexpressed in many forms of RCC (16, 18, 19, 23, 24), and activation of EGFR has been implicated in *VHL*-associated RCC (20, 25, 26). EGF ligands are essential for the proliferation of many human RCC cell lines, and inhibitors of EGFR antagonize RCC cell division in vitro and in vivo (18, 27–29). Clinical trials have demonstrated some efficacy of the EGFR/ErbB2 dual kinase inhibitor lapatinib for advanced-stage RCC (30). However, at present there is no animal model of EGFR-driven RCC; such a model would be valuable for identifying predictors and/or modifiers of clinical response to EGFR-targeted therapies.

In light of the contribution of EGFR to kidney tumorigenesis, the demonstrated role for Merlin/*Nf2* in regulating EGFR, and preliminary evidence implicating mutation of *Nf2* in some RCC patient samples, we hypothesized that *Nf2* mutation would contribute to tumorigenesis from renal tubule epithelial cells in a mouse model. We found that targeted inactivation of *Nf2* in mouse proximal convoluted tubules (PCT), the site of origin for most human RCC, led to multifocal tumor development featuring lumen-filling neoplasia that progressed to invasive carcinoma. These tumors expressed markers characteristic of human RCC and displayed aberrant EGFR signaling and proliferation. In fact, pharmacologic inhibition of EGFR completely halted the proliferation of *Nf2*-deficient renal tumor cells in vivo.

Author contributions: Z.S.M. and A.I.M. designed research; Z.S.M. performed research; Z.S.M. and A.I.M. contributed new reagents/analytic tools; Z.S.M. and A.I.M. analyzed data; and Z.S.M. and A.I.M. wrote the paper.

The authors declare no conflict of interest.

This article is a PNAS Direct Submission.

[1]To whom correspondence should be addressed. E-mail: mcclatch@helix.mgh.harvard.edu.

This article contains supporting information online at www.pnas.org/cgi/content/full/0902031106/DCSupplemental.

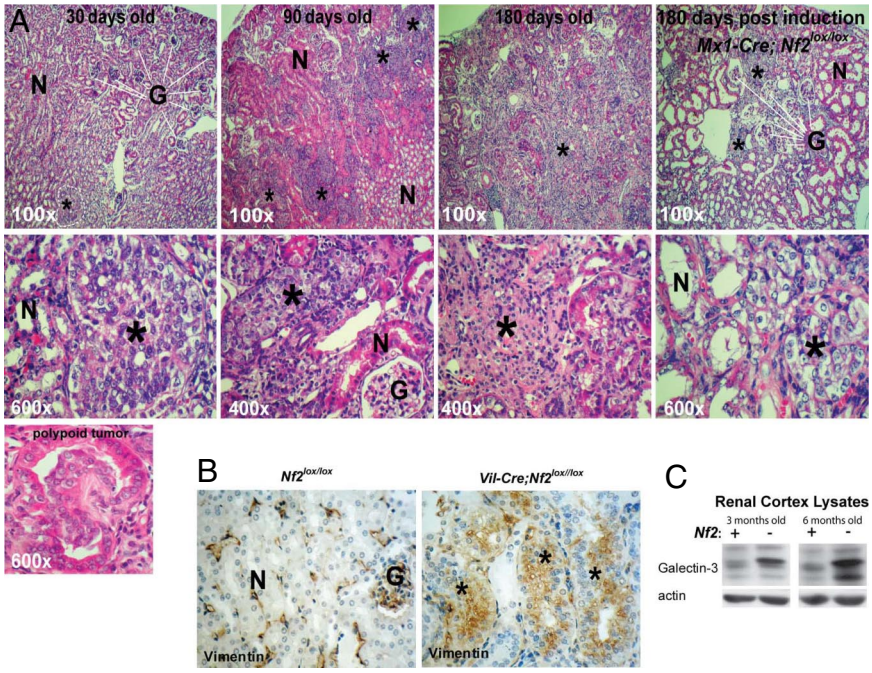

Fig. 1. Targeted loss of *Nf2* in renal tubule epithelia gives rise to vimentin- and galectin-3–positive tumors that progress to invasive carcinoma. (*A*) All *Vil-Cre;Nf2*$^{lox/lox}$ mice developed small intratubular neoplastic growths of atypical epithelial cells by 30 days of age. These grew to large tumors within 3 months and progressed to invasive carcinomas by 6 months. Renal tumors in these mice consistently grew into the tubule lumen, often initiating with a polypoid morphology (*Lower Left*). The *Vil-Cre;Nf2*$^{lox/lox}$ kidney phenotype is recapitulated in inducible *Mx1-Cre;Nf2*$^{lox/lox}$ mice, which target Cre-recombinase expression to the collecting duct (*Right*). (*B*) Tumors in *Vil-Cre;Nf2*$^{lox/lox}$ kidneys stain positive by immunohistochemistry for vimentin. In *Nf2*$^{lox/lox}$ control kidneys vimentin is seen only in glomeruli, arterioles, and interstitial fibroblasts. (*C*) Renal cortex lysates from *Vil-Cre;Nf2*$^{lox/lox}$ mice display increased expression of galectin-3 by immunoblot. Together, vimentin and galectin-3 are histologic markers for clear cell RCC in humans (33). For *A* and *B*, the sections shown are representative of 3 mice × 2 slides per mouse × 3 sections per slide × 2 kidneys per section × ≈10 lesions per kidney = ≈360 lesions examined. N = normal tubules, G = glomeruli. *Lesion/tumor.

Results

To determine whether the loss of *Nf2* can contribute to tumorigenesis in the kidney, we crossed *Nf2*$^{lox/lox}$ mice with *Villin (Vil)-Cre* mice. On the basis of the reported expression of *Vil-Cre*, we expected that these mice would exhibit constitutive loss of *Nf2* in the renal tubule epithelia of the PCT (31). We confirmed this by crossing *Vil-Cre;Nf2*$^{lox/lox}$ mice with mice carrying a *GtRosa26*$^{lox/stop/lox}$ *β-galactosidase* reporter transgene (*R26*$^{LSL\text{-}LacZ}$). Both chemical detection of β-galactosidase activity in whole-mount and paraffin section as well as immunohistochemical labeling using a β-galactosidase–specific antibody revealed Cre activity in the cortical renal tubule epithelia of *Vil-Cre;Nf2*$^{lox/lox}$ mice but not in *Nf2*$^{lox/lox}$ controls [supporting information (SI) Fig. S1 *A* and *B*]. Costaining with the PCT-specific *Lotus tetragonolobus* agglutinin (32) confirmed exclusive targeting of the PCT epithelia (Fig. S1*B*). Immunoblotting of dissected renal cortex lysates revealed a marked reduction in Merlin levels, confirming that we had achieved targeted inactivation of *Nf2* (Fig. S1*C*).

All *Vil-Cre;Nf2*$^{lox/lox}$ mice were runted from birth and occasionally died in the perinatal period between embryonic day 17 and postnatal day 3. *Vil-Cre;Nf2*$^{lox/lox}$ mice that survived until weaning (≈10% of all pups) lived to ≈10 months of age. All of these mice developed lumen-filling intratubular neoplasia by 3 months (Fig. 1*A*). Lesions were apparent as early as 15 days of age and most commonly initiated in the corticomedullary junction as projections of atypical epithelial cells into the PCT lumen (Fig. 1*A*). By 6 months the size and number of tumors was greatly increased, displacing large areas of normal renal tissue and penetrating tubule basement membrane as invasive carcinomas. Heterozygous *Vil-Cre;Nf2*$^{lox/+}$ mice, on the other hand, were indistinguishable from *Nf2*$^{lox/lox}$ controls (not shown). Renal tumors in *Vil-Cre;Nf2*$^{lox/lox}$ mice stained positive for vimentin (Fig. 1*B*). Immunoblotting of kidney cortex lysate indicated that these lesions were also galectin-3 positive (Fig. 1*C*). Vimentin and galectin-3 are established markers of clear cell RCC in humans (33).

To ascertain whether renal tubule tumors that develop in *Vil-Cre;Nf2*$^{lox/lox}$ mice derive from a developmentally and/or regionally specific cell population, we deleted *Nf2* in the adult kidney using the IFN-α–inducible *Mx1-Cre* transgene. The *Mx1* promoter drives Cre-recombinase activity in epithelial cells of the collecting duct and the thick ascending loop of Henle in the nephron but not in the PCT (34). *Mx1-Cre;Nf2*$^{lox/lox}$ mice also developed lumen-filling renal tubule neoplasia within 6 months of *Mx1-Cre* induction (Fig. 1*A*). Consistent with the distal location of these lesions in the nephron, kidneys of *Mx1-Cre;Nf2*$^{lox/lox}$ mice displayed dilation of upstream tubules upon tumor development, likely due to blocked urinary flow. This was understandably not prominent in *Vil-Cre;Nf2*$^{lox/lox}$ mice, which developed more proximal tumors in the PCT. Nevertheless, the development of morphologically similar lesions in *Vil-Cre;Nf2*$^{lox/lox}$ and *Mx1-Cre;Nf2*$^{lox/lox}$ mice suggests that Merlin is an essential regulator of proliferation across the renal tubule epithelium and further supports the notion that somatic loss of *Nf2* may contribute to sporadic renal tumorigenesis in humans.

Very few cells are proliferating in the normal adult mouse kidney. In contrast, renal tubule carcinomas in *Vil-Cre;Nf2*$^{lox/lox}$ mice were hyperproliferative, displaying a greater than 7-fold increase in Ki67- and phosphorylated histone 3 (PH3)-positive nuclei and in the number of nuclei labeled by BrdU during a short 3-h premortem labeling (Fig. 2 *A* and *B*; data not shown). In addition, *Vil-Cre;Nf2*$^{lox/lox}$ kidneys exhibited a marked increase in the number of BrdU label-retaining putative progenitor cells (35–37) during a 1-week pulse/2-week chase experiment (Fig. 2 *C* and *D*). Notably, this increase in proliferation was accompanied by a dramatic increase in phosphotyrosine levels within both early and late lesions (Fig. 3*A*). Immunoblotting demonstrated strong and progressive activation of EGFR, its principle dimerization partner ErbB2, and its downstream targets Akt, MAPK, and STAT-3 (Fig. 3*B*). Immunohistochemistry confirmed that the activation of these targets was restricted to *Nf2*-deficient tumors (Fig. 3*C*). Importantly, we did *not* detect significant differences in the expression of EGF ligands in *Nf2*$^{lox/lox}$ and *Vil-Cre;Nf2*$^{lox/lox}$ kidneys (Fig. S2*A*).

We previously found that Merlin is critical for the establishment of stable AJs in several types of cultured cells (22). Intriguingly, although equivalent levels of core AJ components were present in renal cortical lysates derived from *Nf2*$^{lox/lox}$ and *Vil-Cre;Nf2*$^{lox/lox}$ kidneys, we noted a striking difference in their detergent solubility in the absence of Merlin (Fig. 4*A*). Both p120- and β-catenin exhibited greatly enhanced detergent solubility in *Vil-Cre;Nf2*$^{lox/lox}$ kidneys. This could be consistent with a failure to stabilize these

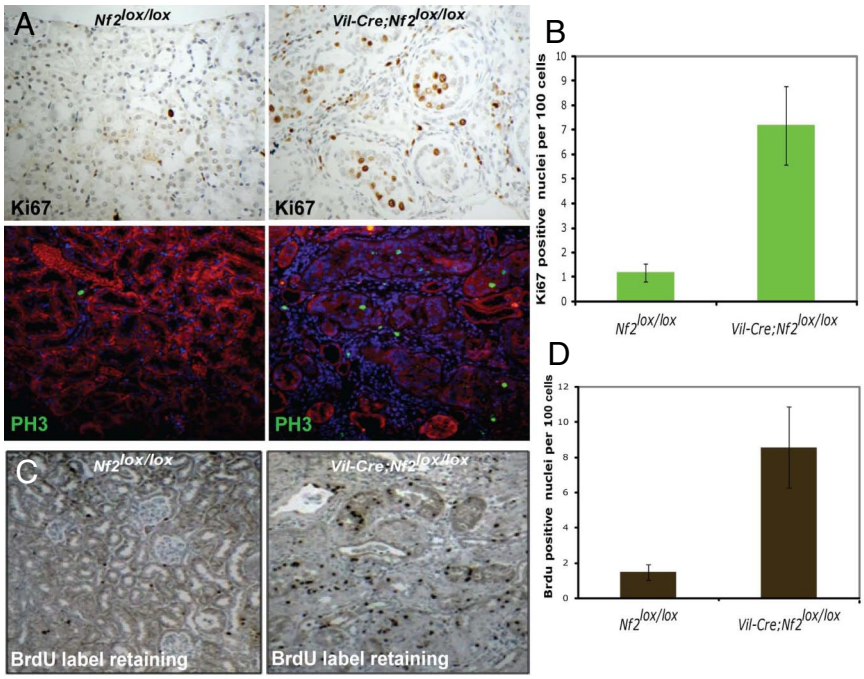

Fig. 2. *Vil-Cre;Nf2*$^{lox/lox}$ kidneys display heightened epithelial cell proliferation and an increased number of label-retaining putative progenitor cells. (*A*) Three-month-old *Vil-Cre;Nf2*$^{lox/lox}$ kidneys displayed increased proliferation of cells mostly localized to lumen-filling neoplastic growths, as measured by nuclear staining of Ki67 (immunohistochemistry) and PH3 (green, immunofluorescence). Renal epithelial cells are displayed in red on immunofluorescence images. (*B*) Quantification per 100 cells revealed a ≈7-fold increase in Ki67-positive nuclei in the *Vil-Cre;Nf2*$^{lox/lox}$ renal cortex relative to controls. (*C* and *D*) BrdU pulse–chase experiments (1-week pulse, 2-week chase), previously reported to identify putative progenitor cells (57), demonstrated a ≈5-fold increase in the number of label-retaining cells in the *Vil-Cre;Nf2*$^{lox/lox}$ renal cortex relative to controls. The sections shown are representative of multiple mice, sections, and lesions as defined in the legend to Fig. 1.

proteins at the insoluble, cytoskeleton-associated AJ complex in the absence of Merlin. Indeed, immunohistochemical staining demonstrated that β-catenin was not strongly localized to cell–cell contacts in *Nf2*-deficient lesions (Fig. 4*B*). Interestingly, given the purported necessity of AJs in establishing apico-basolateral polarity (38–40), we also found that cells within *Vil-Cre;Nf2*$^{lox/lox}$ neoplastic tissues failed to properly localize the apical markers ezrin and Na/H exchanger regulatory factor (NHERF)-1 and the apical tight junction marker ZO-1 (Fig. 4*C*, Fig. S2*B*). Notably, increased EGFR signaling was not separated temporally from altered localization of junctional proteins and polarity markers, and these effects of *Nf2* deficiency were apparent in the earliest detectable lesions in 2-week-old *Vil-Cre;Nf2*$^{lox/lox}$ mice (not shown).

To further investigate the cellular and molecular effects of *Nf2* deficiency in renal tubule epithelial cells, we derived primary epithelial cell cultures from the renal cortex of *Nf2*$^{lox/lox}$, *Vil-Cre;Nf2*$^{lox/lox}$, and IFN-induced *Mx1-Cre;Nf2*$^{lox/lox}$ mice. Only cells from *Vil-Cre;Nf2*$^{lox/lox}$ and *Mx1-Cre;Nf2*$^{lox/lox}$ cortex grew to confluence and survived passaging (Fig. S3*A*). Like other *Nf2*$^{-/-}$ cells, *Nf2*-deficient kidney epithelial cells failed to undergo contact-dependent inhibition of proliferation, a phenotype that was reversed by viral re-expression of *Nf2* (Fig. S3 *B–D*). Notably, we also found that *Nf2*-deficient renal epithelial cells required EGF for growth in culture and were strongly and reversibly growth suppressed by treatment with the EGFR tyrosine kinase inhibitor erlotinib (Fig. S3 *C* and *D*). Remarkably, *Nf2*-deficient renal

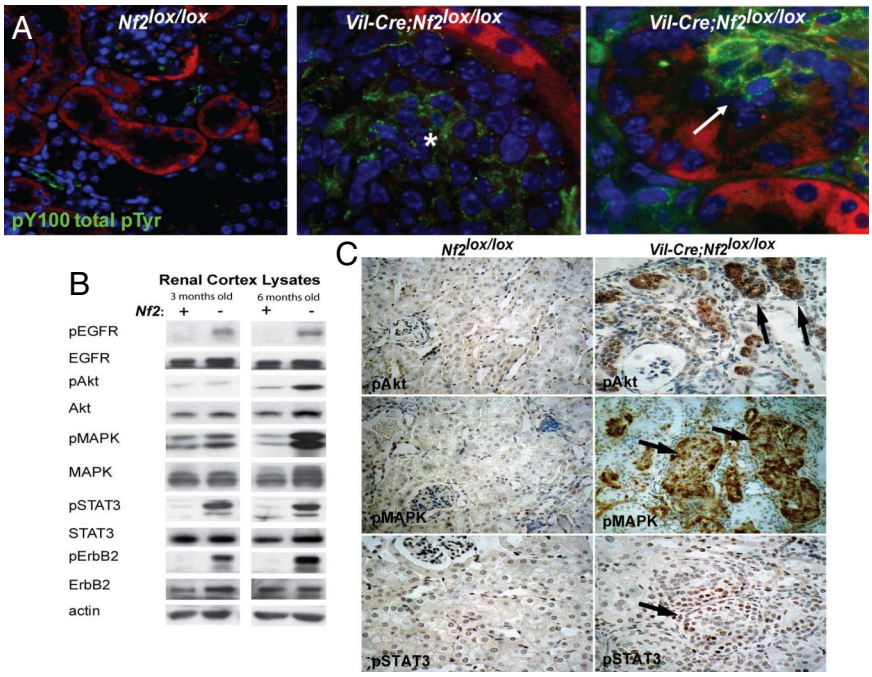

Fig. 3. Tumors in *Vil-Cre;Nf2*$^{lox/lox}$ kidneys are foci of activated EGFR signaling. (*A*) Immunofluorescent detection using the pY100 antibody (green) revealed a marked increase in phosphotyrosine signaling in early (*Right*) and late (*Middle*) lesions in *Vil-Cre;Nf2*$^{lox/lox}$ kidneys. Renal epithelial cells are displayed in red. (*B*) Immunoblot demonstrated activation of EGFR, its preferred dimerization partner ErbB2, and its downstream effectors in renal cortex lysates from 3- and 6-month-old *Vil-Cre;Nf2*$^{lox/lox}$ mice. (*C*) Immunohistochemical detection of phosphorylated Akt, MAPK, and STAT-3 in paraffin sections of 3-month-old kidneys demonstrated that hyperactivation of these EGFR effectors was confined to neoplastic lesions in *Vil-Cre;Nf2*$^{lox/lox}$ mice. The sections shown are representative of multiple mice, sections and lesions as defined in the legend to Fig. 1.

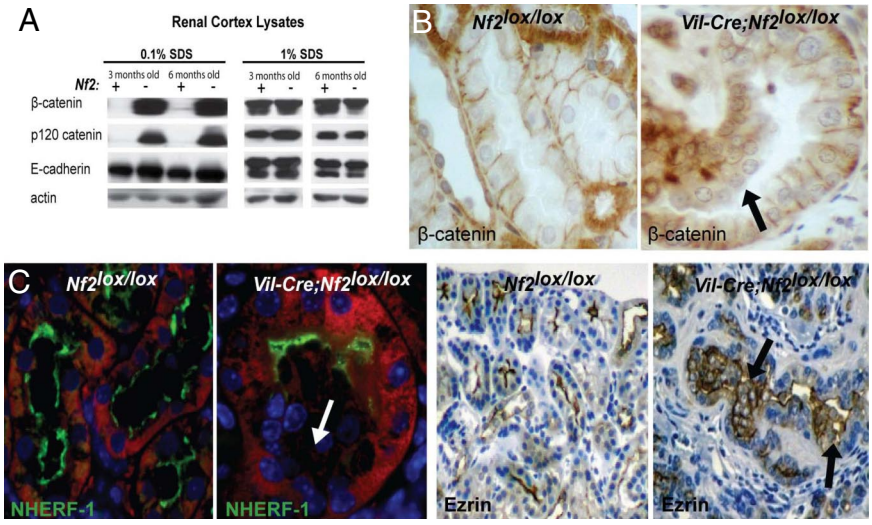

Fig. 4. Tumor cells in *Vil-Cre;Nf2*$^{lox/lox}$ kidneys exhibit increased solubility of AJ components and a loss of polarity. (*A*) Rigorous 1% SDS solubilization demonstrated equivalent expression of AJ components. A gentler 0.1% SDS solubilization revealed stark differences in the solubility of the AJ components, p120- and β-catenin, between *Vil-Cre;Nf2*$^{lox/lox}$ and *Nf2*$^{lox/lox}$ kidney lysates. (*B*) Immunohistochemical staining demonstrated that this change in solubility correlated with a loss of β-catenin localization to cell–cell contacts in neoplastic cells of 3-month-old *Vil-Cre;Nf2*$^{lox/lox}$ mice. (*C*) Histologic examination of the apical markers NHERF-1 (green, immunofluorescence) and ezrin (immunohistochemistry) showed a loss of cell polarity in early intratubule growths arising in *Vil-Cre;Nf2*$^{lox/lox}$ kidneys. Renal epithelial cells are displayed in red on immunofluorescence images. The sections shown are representative of multiple mice, sections, and lesions as defined in the legend to Fig. 1.

epithelial cells were capable of forming malignant s.c. tumors in nude mice without in vitro passage (Fig. S3 *E* and *F*). These tumors displayed an intriguing mixed histology, with some areas seeming to regenerate a tubular architecture that was compromised by lumen filling.

Collectively, these data suggested that aberrant EGFR signaling may underlie the tumorigenic consequences of *Nf2* deficiency in the kidney epithelium in vivo. To test this hypothesis, we treated 12–16-week old *Vil-Cre;Nf2*$^{lox/lox}$ mice with erlotinib by i.p. injection, twice daily for 10 days. Erlotinib treatment completely halted the over-proliferation of renal tumor cells within these mice, restoring wild-type levels of Ki67- and PH3-positive nuclei (Fig. 5*A*). This was associated with decreased activation of classic downstream signaling effectors, such as Akt, MAPK, and STAT-3; notably, erlotinib also reduced the activation of nonclassic EGFR effectors, such as caveolin-1 (Fig. 5 *B* and *C*). Consistent with the cytostatic effects observed in vitro (Fig. S3 *C* and *D*), erlotinib treatment did not induce apoptosis or necrosis in renal tumors from *Vil-Cre;Nf2*$^{lox/lox}$ mice (not shown).

Discussion

In this work we present a genetically engineered mouse model of renal epithelial cell tumorigenesis. The *Vil-Cre;Nf2*$^{lox/lox}$ mouse joins a short list of genetically defined models of RCC and is the first to recapitulate the activation of EGFR signaling that is often reported in human RCC. Targeted loss of the *Nf2* tumor suppressor in renal tubule epithelial cells gives rise to tumor development with 100% penetrance. Lesions within the *Nf2*-deficient renal tubule epithelia develop via a reproducible progression from lumen-filling intratubular neoplasia that develops over the course of 3 to 4 months to invasive carcinoma by 6–10 months. These tumors display histologic features and express markers that are diagnostic of human clear cell RCC. Treatment of these mice with the EGFR tyrosine kinase inhibitor erlotinib demonstrated that EGFR signaling was necessary for the over-proliferation observed in these tumors. *Nf2*-deficient epithelial cells derived from early or late lesions in these kidneys do not undergo contact-dependent inhibition of proliferation but are antagonized by pharmacologic inhibition of EGFR signaling. These cells can be passaged repeatedly in culture but, remarkably, are capable of generating malignant tumors upon s.c. injection into immunocompromised mice before in vitro passage. This mouse model and cells derived from it may therefore prove useful for examining in vivo mechanisms of resistance or sensitivity to EGFR-targeted therapeutics in the kidney. The robust activation of downstream EGFR signaling pathways in

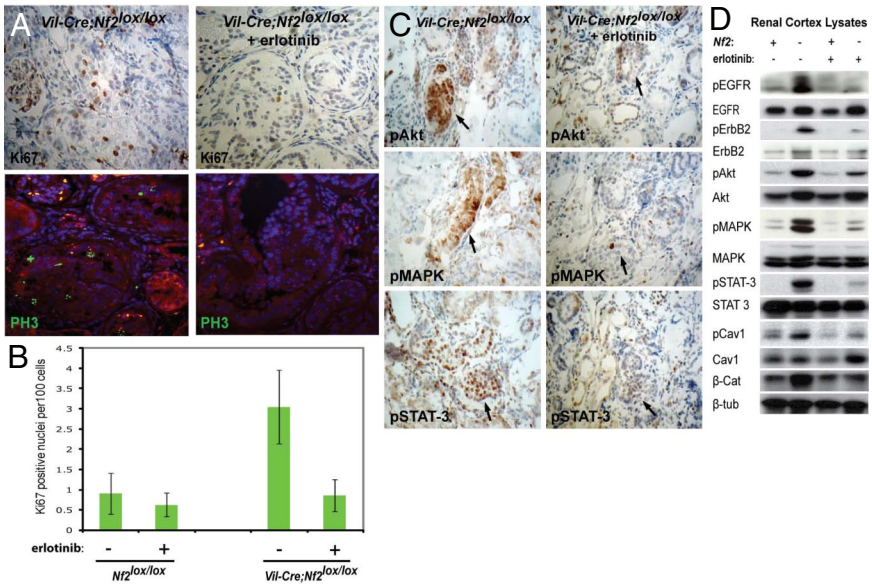

Fig. 5. Erlotinib treatment of *Vil-Cre;Nf2*$^{lox/lox}$ mice restores wild-type levels of proliferation to *Nf2*-deficient renal tubule epithelia. (*A* and *B*) Twelve- to 16-week-old *Vil-Cre;Nf2*$^{lox/lox}$ mice were treated by i.p. injection of 100 mg/kg erlotinib twice daily for 10 days. Erlotinib treatment restored wild-type levels of proliferation in *Vil-Cre;Nf2*$^{lox/lox}$ mice, as assayed by quantification of Ki67 (immunohistochemistry) and PH3 (green, immunofluorescence) positive nuclei per 100 cells. Statistical significance was determined by one-tailed, independent samples, parametric *t* test, $P = 0.00085$. (*C*) Renal tumors in erlotinib-treated mice exhibited decreased activation of EGFR signaling effectors by immunohistochemistry. The sections shown are representative of multiple mice, sections, and lesions as defined in the legend to Fig. 2. (*D*) Immunoblot of 0.1% SDS renal cortex lysates confirmed decreased activation of EGFR, its dimerization partner ErbB2, and its downstream effectors in erlotinib treated *Vil-Cre;Nf2*$^{lox/lox}$ mice as compared with untreated controls. Interestingly, targeting EGFR signaling also seemed to normalize the solubility of β-catenin.

this model will provide an excellent metric for exploring and quantifying the molecular effects of such interventions.

The *Vil-Cre;Nf2*$^{lox/lox}$ mouse gives added credence to the role of the EGFR pathway in RCC and provides an excellent tool for investigating the molecular mechanisms that contribute to EGFR-dependent tumorigenesis in the kidney. We previously reported that persistent EGFR signaling drives the loss of contact-dependent inhibition of proliferation exhibited by primary cultured *Nf2*-deficient cells of several different types (17, 21). Here we demonstrate a causal role for aberrant EGFR signaling in *Nf2*-associated tumorigenesis in vivo. In cultured cells, Merlin antagonizes EGFR signaling in a contact-dependent manner by coordinating the establishment of stable AJs with inhibition of EGFR internalization, thereby limiting access of EGFR to its downstream effectors (17, 22). In addition to the canonical EGFR effectors, we found that *Nf2*-deficient kidney lysates exhibit markedly elevated levels of phosphorylated caveolin-1 (Fig. 5*C*), which is downstream of EGFR activation and permissive to caveolae-mediated endocytosis, 1 of 2 major routes of EGFR internalization (41–43). This supports the notion that Merlin can also regulate EGFR endocytosis in vivo. Here we also present evidence that Merlin stabilizes AJs in vivo as it does in cell culture (22). Thus, in contrast to membrane-bound E-cadherin, both p120- and β-catenin fail to localize to a biochemically insoluble subcellular compartment in the absence of Merlin (Fig. 4*A*). This could reflect a failure to link E-cadherin tetramers to the insoluble cytoskeleton and thereby form mature AJs.

Although clinical trials that examined the efficacy of EGFR inhibitors in RCC were largely disappointing, the dual EGFR/ErbB2 kinase inhibitor lapatinib has shown efficacy against therapy-resistant RCC tumors that over-express EGFR (30). Notably, EGFR is capable of signaling from heterodimeric EGFR–ErbB2 complexes in the renal epithelium and, although rare, co-overexpression of these 2 proteins is associated with poor outcome in RCC (44, 45). We found markedly increased phosphorylation of both EGFR and ErbB2 in the *Vil-Cre;Nf2*$^{lox/lox}$ renal cortex, suggesting that Merlin antagonizes activation of ErbB2, perhaps via regulation of EGFR–ErbB2 heterodimers. Perhaps retrospective analyses will reveal *NF2* deficiency or deregulation as a predictor of patient response to lapatinib in RCC. Interestingly, in 3-dimensional mammary epithelial cultures, aberrant ErbB2 activity drives loss of polarity and lumen filling (46), both of which are prominent features of the early lesions that develop in the *Nf2*-deficient kidney. Together with the known role of AJs in the establishment of apico-basolateral cell polarity (38, 39), these observations may suggest a broader role for Merlin in coordinating ErbB signaling with the establishment of cell polarity in vivo. Notably, we also observe EGFR-dependent hyperactivation of Akt in the renal cortex of *Vil-Cre;Nf2*$^{lox/lox}$ mice. Akt signaling can be proximally regulated by PI3-kinase, mammalian target of rapamycin, and phosphatase and tensin homolog (PTEN)—each of which contributes to RCC when disrupted (47–50). This mouse model may further support the importance of Akt signaling in RCC and be useful in studying the tumorigenic effects of this pathway.

Preliminary data from patient samples in the Sanger COSMIC database suggest that *NF2* may be disrupted in some cases of sporadic RCC (15). Our findings warrant a more rigorous investigation of this possibility across a large set of sporadic RCC tumors. The absence of a clear increase in kidney tumor susceptibility in NF2 patients could reflect the fact that NF2 is rare and compromises life expectancy in most patients before the average age of onset of RCC. Alternatively, additional cooperating mutations may be necessary for *NF2*-driven RCC in humans, where somatic inactivation of *NF2* likely occurs in individual cells in an otherwise wild-type or heterozygous-mutant epithelium. In fact, this model may be valuable in identifying such cooperating mutations.

Although we targeted loss of *Nf2* in renal epithelia throughout entire regions of the nephron, we commonly observed polypoid tumor formation, often initially surrounded by normal-looking epithelial cells (Fig. 1). The pervasive expression and activity of a Rosa26-driven β-galactosidase reporter across the epithelium targeted by both *Villin*- and *Mx1*-Cre transgenes argues against the possibility that this reflects selective excision of *Nf2* in a few cells of the renal epithelial monolayer. Similarly, the rapid onset and multiplicity of early lesions suggests that cooperating events are not required for the initiation of tumorigenesis in this model. Alternatively, the observation of polypoid tumors surrounded by apparently normal *Nf2*-deficient epithelial cells may suggest that a specific cell of origin is preferentially affected by loss of *Nf2*. Mounting evidence from targeted inactivation of *Nf2* in other tissues suggests that tissue progenitor cells are particularly sensitive to loss of Merlin (M. Curto, S. Benhamouche, A. Gladden, and A.I.M., unpublished data). In fact, *Nf2* deficiency results in a dramatic increase in the number of label-retaining putative progenitor cells in the kidney, and polypoid tumors in the *Nf2*-deficient renal epithelium initiate at the corticomedullary junction, a region thought to harbor the progenitor cell niche in the adult kidney (35–37). It is tempting to speculate that a kidney progenitor cell is particularly sensitive to loss of Merlin-mediated, contact-dependent inhibition of proliferation in vivo and that this is the cell of origin of RCC in this model and perhaps in some cases of human RCC.

Materials and Methods

SI Materials and Methods provides further details.

Animals and Animal Procedures. Homozygous *Nf2*$^{lox/lox}$ mice were kindly provided by M. Giovannini (51) and crossed with transgenic mice expressing the Cre recombinase under the *Villin* promoter (*Vil-Cre*) kindly provided by S. Robine (31) or the IFN-α–inducible *Mx1* promoter (*Mx1-Cre*) [*Tg(Mx1-Cre)1Cgn/J*; Jackson Laboratory] (52). To monitor Cre-mediated excision, mice were crossed to *R26*$^{LSL-LacZ}$ [B6;129-*Gt(ROSA)26Sor*^{tm1Sho}/J; Jackson Laboratory] reporter mice (53). Immunocompromised 5-week-old female *nu/nu* mice were obtained from the Massachusetts General Hospital (MGH) Cox7 facility.

Erlotinib (ChemieTek) was solubilized at 10 mg/mL in a 6% wt/vol aqueous solution of Captisol (CyDex Pharmaceuticals). Four *Vil-Cre;Nf2*$^{lox/lox}$ and 4 *Nf2*$^{lox/lox}$ control mice were treated by i.p. injection of erlotinib at 100 mg/kg body weight once every 12 h for 10 days. Two *Vil-Cre;Nf2*$^{lox/lox}$ and 2 *Nf2*$^{lox/lox}$ control mice were treated on the same schedule with vehicle alone, with no detectable effect. We chose to treat mice at an age (12–16 weeks) when all had developed a significant tumor burden but no tumors had acquired invasive characteristics. At this early stage, tumors were also not vascularized, and neither apoptosis nor necrosis was detectable. All animal procedures were performed according to federal and institutional guidelines and approved by the MGH Subcommittee on Research Animal Care.

Histology and Immunohistochemistry. Sections were incubated overnight at 4 °C with the following primary antibodies: BD Biosciences (β-catenin, 1:500, #610154), Cell Signaling (anti-pAkt, 1:50, #4060; Anti-pMAPK, 1:200, #4370; and Anti-pSTAT3, 1:50, #9145), Neomarkers (anti-Ezrin, 1:200, #3C12; and anti-Vimentin, 1:400, V9), and Novocastra (anti-Ki67, 1:200). BrdU-labeled cells were detected using a kit (Zymed) according to the manufacturer's instructions. HRP-conjugated secondary antibodies (used for Ezrin, Vimentin, and Ki67) were detected using the DAB peroxidase substrate kit (Vector Laboratories). Biotinylated secondary antibodies (for β-catenin, pAkt, pMAPK, and pSTAT3) were detected using the ABC immunoperoxidase kit (Vector Laboratories).

Immunofluorescence. Paraffin sections were incubated overnight at 4 °C with the following primary antibodies: Cell Signaling (PH3, 1:200, #9701; and P-Y100, 1:1,000, #9411), Abcam (NHERF-1, 1:200, #3452), and Zymed (anti-ZO-1, 1:60). Primary antibodies were detected using Alexa Fluor 488 secondary antibodies (Invitrogen), and slides were costained with DAPI and mounted (Vectashield; Vector Laboratories). Renal epithelial cells were visualized by autofluorescence at 594 nm in paraffin sections. Cryosections were incubated at 37 °C (30 min) with biotinylated *Lotus tetragonolobus* agglutinin (1:80 from stock solution; Vector Laboratories). Sections were subsequently incubated overnight at 4 °C with anti-β-galactosidase (1:500, Cappel #55976). FITC–streptavidin and Alexa Fluor 594 secondary antibodies were used for detection, and slides were costained with DAPI. Images were acquired as z-stacks on an Olympus 1 × 81 spinning disk confocal microscope with a Hamamatsu EM CCD digital camera and processed using Slidebook imaging software (Olympus) and Photoshop CS4 (Adobe Systems).

Immunoblotting. Proteins were detected using the following primary antibodies: Cell Signaling (pEGFR, #2235; pSTAT-3, #9145; STAT-3, #4904; pAkt, #4060; Akt, #4685; pMAPK, #4370; MAPK, #4696; pErbB2, #2243; and TGF-α, #3175, all at 1:1,000), Santa Cruz Biotechnology (NF2, #sc-331, 1:2,000; ErbB2, #sc-284; and EGFR, #sc-03, both at 1:1,000; and HB-EGF, #sc-21593, 1:200), BD Biosciences (E-cadherin, #610182; p120 catenin, #610134; and Caveolin-1, #610407, all at 1:2,000; β-catenin, #610154, 1:500; and pCaveolin, #611339, 1:1,000), Sigma (actin, AC40, 1:4,000; and β-tubulin, #SAP-4G5, 1:500), Abcam (Galectin-3, #A3A12, 1:1,000), and Neomarkers (amphiregulin, AB-1, 1:200). HRP-conjugated secondary antimouse and antirabbit antibodies were from Amersham.

Primary Cultures. Primary cultures of renal epithelial cells were generated by dissection of PBS-flushed kidneys using modified protocols (54, 55). Where indicated, cells were treated with 1 μM erlotinib or DMSO overnight. Mouse wild-type *Nf2* cDNA was cloned into a puromycin-selectable retroviral pBabe vector from a previously described plasmid (22). Cells were infected, selected, and passaged once before experiments. To evaluate contact-inhibition of cell-cycle progression, confluent cells were trypsinized, washed in PBS, fixed overnight at -20 °C in 70% ethanol, stained for 30 min with propidium iodide (10 μg/mL in PBS), and analyzed by FACS to evaluate DNA content. For xenograft experiments, immunocompromised mice were injected s.c. with 1×10^6 prepassage cells (isolated, plated, and grown to confluence) that had been trypsinized, washed in PBS with 0.1% soy trypsin inhibitor, and resuspended in PBS.

ACKNOWLEDGMENTS. We thank Marco Giovannini and Sylvie Robine for *Nf2*$^{lox/lox}$ and *Villin-Cre* mice, respectively; Othon Iliopoulos, Jordan Kreidberg, and Marcello Curto for advice and discussion; Rod Bronson, Sabina Signoretti, and Chin-Lee Wu for pathology consultation; and Andrew Gladden and Brett Morris for assistance with FACS and immunohistochemistry, respectively. This work was supported by National Institutes of Health (NIH)/National Cancer Institute Grant CA113733 (to A.I.M.); NIH/National Institute of General Medical Sciences Grant T32 GM07306 (to Z.S.M.); and Department of Defense Grant W81XWH-05–1-0189 (to A.I.M.).

1. Cohen HT, McGovern FJ (2005) Renal-cell carcinoma. *N Engl J Med* 353:2477–2490.
2. Valladares Ayerbes M, et al. (2008) Origin of renal cell carcinomas. *Clin Transl Oncol* 10:697–712.
3. Iliopoulos O (2006) Molecular biology of renal cell cancer and the identification of therapeutic targets. *J Clin Oncol* 24:5593–5600.
4. Motzer RJ, Bander NH, Nanus DM (1996) Renal-cell carcinoma. *N Engl J Med* 335:865–875.
5. Takahashi M, Kahnoski R, Gross D, Nicol D, Teh BT (2002) Familial adult renal neoplasia. *J Med Genet* 39:1–5.
6. Kleymenova E, et al. (2004) Susceptibility to vascular neoplasms but no increased susceptibility to renal carcinogenesis in Vhl knockout mice. *Carcinogenesis* 25:309–315.
7. Graveel C, et al. (2004) Activating Met mutations produce unique tumor profiles in mice with selective duplication of the mutant allele. *Proc Natl Acad Sci USA* 101:17198–17203.
8. Pollard PJ, et al. (2007) Targeted inactivation of fh1 causes proliferative renal cyst development and activation of the hypoxia pathway. *Cancer Cell* 11:311–319.
9. Kobayashi T, et al. (2001) A germ-line Tsc1 mutation causes tumor development and embryonic lethality that are similar, but not identical to, those caused by Tsc2 mutation in mice. *Proc Natl Acad Sci USA* 98:8762–8767.
10. Kobayashi T, et al. (1999) Renal carcinogenesis, hepatic hemangiomatosis, and embryonic lethality caused by a germ-line Tsc2 mutation in mice. *Cancer Res* 59:1206–1211.
11. Baba M, et al. (2008) Kidney-targeted Birt-Hogg-Dube gene inactivation in a mouse model: Erk1/2 and Akt-mTOR activation, cell hyperproliferation, and polycystic kidneys. *J Natl Cancer Inst* 100:140–154.
12. Chen J, et al. (2008) Deficiency of FLCN in mouse kidney led to development of polycystic kidneys and renal neoplasia. *PLoS ONE* 3:e3581.
13. Qian CN, et al. (2005) Cystic renal neoplasia following conditional inactivation of apc in mouse renal tubular epithelium. *J Biol Chem* 280:3938–3945.
14. Sansom OJ, Griffiths DF, Reed KR, Winton DJ, Clarke AR (2005) Apc deficiency predisposes to renal carcinoma in the mouse. *Oncogene* 24:8205–8210.
15. Forbes SA, et al. (2008) The Catalogue of Somatic Mutations in Cancer (COSMIC). *Curr Protoc Hum Genet* Chapter 10:Unit 10.11.
16. Uhlman DL, et al. (1995) Epidermal growth factor receptor and transforming growth factor alpha expression in papillary and nonpapillary renal cell carcinoma: Correlation with metastatic behavior and prognosis. *Clin Cancer Res* 1:913–920.
17. Curto M, Cole BK, Lallemand D, Liu CH, McClatchey AI (2007) Contact-dependent inhibition of EGFR signaling by Nf2/Merlin. *J Cell Biol* 177:893–903.
18. Moch H, et al. (1997) Epidermal growth factor receptor expression is associated with rapid tumor cell proliferation in renal cell carcinoma. *Hum Pathol* 28:1255–1259.
19. Merseburger AS, et al. (2005) Membranous expression and prognostic implications of epidermal growth factor receptor protein in human renal cell cancer. *Anticancer Res* 25:1901–1907.
20. Smith K, et al. (2005) Silencing of epidermal growth factor receptor suppresses hypoxia-inducible factor-2-driven VHL-/- renal cancer. *Cancer Res* 65:5221–5230.
21. Cole BK, Curto M, Chan AW, McClatchey AI (2008) Localization to the cortical cytoskeleton is necessary for Nf2/merlin-dependent epidermal growth factor receptor silencing. *Mol Cell Biol* 28:1274–1284.
22. Lallemand D, Curto M, Saotome I, Giovannini M, McClatchey AI (2003) NF2 deficiency promotes tumorigenesis and metastasis by destabilizing adherens junctions. *Genes Dev* 17:1090–1100.
23. Ananth S, et al. (1999) Transforming growth factor beta1 is a target for the von Hippel-Lindau tumor suppressor and a critical growth factor for clear cell renal carcinoma. *Cancer Res* 59:2210–2216.
24. Franovic A, et al. (2007) Translational up-regulation of the EGFR by tumor hypoxia provides a nonmutational explanation for its overexpression in human cancer. *Proc Natl Acad Sci USA* 104:13092–13097.
25. de Paulsen N, et al. (2001) Role of transforming growth factor-alpha in von Hippel-Lindau (VHL)(-/-) clear cell renal carcinoma cell proliferation: A possible mechanism coupling VHL tumor suppressor inactivation and tumorigenesis. *Proc Natl Acad Sci USA* 98:1387–1392.
26. Gunaratnam L, et al. (2003) Hypoxia inducible factor activates the transforming growth factor-alpha/epidermal growth factor receptor growth stimulatory pathway in VHL(-/-) renal cell carcinoma cells. *J Biol Chem* 278:44966–44974.
27. Prewett M, et al. (1998) Mouse-human chimeric anti-epidermal growth factor receptor antibody C225 inhibits the growth of human renal cell carcinoma xenografts in nude mice. *Clin Cancer Res* 4:2957–2966.
28. Rowinsky EK, et al. (2004) Safety, pharmacokinetics, and activity of ABX-EGF, a fully human anti-epidermal growth factor receptor monoclonal antibody in patients with metastatic renal cell cancer. *J Clin Oncol* 22:3003–3015.
29. Foon KA, et al. (2004) Preclinical and clinical evaluations of ABX-EGF, a fully human anti-epidermal growth factor receptor antibody. *Int J Radiat Oncol Biol Phys* 58:984–990.
30. Ravaud A, et al. (2008) Lapatinib versus hormone therapy in patients with advanced renal cell carcinoma: A randomized phase III clinical trial. *J Clin Oncol* 26:2285–2291.
31. el Marjou F, et al. (2004) Tissue-specific and inducible Cre-mediated recombination in the gut epithelium. *Genesis* 39:186–193.
32. Faraggiana T, Malchiodi F, Prado A, Churg J (1982) Lectin-peroxidase conjugate reactivity in normal human kidney. *J Histochem Cytochem* 30:451–458.
33. Young AN, et al. (2001) Expression profiling of renal epithelial neoplasms: A method for tumor classification and discovery of diagnostic molecular markers. *Am J Pathol* 158:1639–1651.
34. Schneider A, Zhang Y, Guan Y, Davis LS, Breyer MD (2003) Differential, inducible gene targeting in renal epithelia, vascular endothelium, and viscera of Mx1Cre mice. *Am J Physiol Renal Physiol* 284:F411–F417.
35. Sakakima M, Fujigaki Y, Yamamoto T, Hishida A (2008) A distinct population of tubular cells in the distal S3 segment contributes to S3 segment regeneration in rats following acute renal failure induced by uranyl acetate. *Nephron Exp Nephrol* 109:e57–e70.
36. Kim K, Lee KM, Han DJ, Yu E, Cho YM (2008) Adult stem cell-like tubular cells reside in the corticomedullary junction of the kidney. *Int J Clin Exp Pathol* 1:232–241.
37. Maeshima A (2007) Label-retaining cells in the kidney: Origin of regenerating cells after renal ischemia. *Clin Exp Nephrol* 11:269–274.
38. Caplan MJ, Seo-Mayer P, Zhang L (2008) Epithelial junctions and polarity: Complexes and kinases. *Curr Opin Nephrol Hypertens* 17:506–512.
39. Capaldo CT, Macara IG (2007) Depletion of E-cadherin disrupts establishment but not maintenance of cell junctions in Madin-Darby canine kidney epithelial cells. *Mol Biol Cell* 18:189–200.
40. Suzuki A, Ohno S (2006) The PAR-aPKC system: Lessons in polarity. *J Cell Sci* 119(Pt 6):979–987.
41. Sigismund S, et al. (2005) Clathrin-independent endocytosis of ubiquitinated cargos. *Proc Natl Acad Sci USA* 102:2760–2765.
42. Kim YN, Wiepz GJ, Guadarrama AG, Bertics PJ (2000) Epidermal growth factor-stimulated tyrosine phosphorylation of caveolin-1. Enhanced caveolin-1 tyrosine phosphorylation following aberrant epidermal growth factor receptor status. *J Biol Chem* 275:7481–7491.
43. Sverdlov M, Shajahan AN, Minshall RD (2007) Tyrosine phosphorylation-dependence of caveolae-mediated endocytosis. *J Cell Mol Med* 11:1239–1250.
44. Wilson SJ, et al. (2006) Inhibition of HER-2(neu/ErbB2) restores normal function and structure to polycystic kidney disease (PKD) epithelia. *Biochim Biophys Acta* 1762:647–655.
45. Latif Z, Watters AD, Bartlett JM, Underwood MA, Aitchison M (2002) Gene amplification and overexpression of HER2 in renal cell carcinoma. *BJU Int* 89:5–9.
46. Muthuswamy SK, Li D, Lelievre S, Bissell MJ, Brugge JS (2001) ErbB2, but not ErbB1, reinitiates proliferation and induces luminal repopulation in epithelial acini. *Nat Cell Biol* 3:785–792.
47. Hager M, et al. (2008) Increased activated Akt expression in renal cell carcinomas and prognosis. *J Cell Mol Med*, in press.
48. Merseburger AS, et al. (2008) Activation of PI3K is associated with reduced survival in renal cell carcinoma. *Urol Int* 80:372–377.
49. Pantuck AJ, et al. (2007) Prognostic relevance of the mTOR pathway in renal cell carcinoma: Implications for molecular patient selection for targeted therapy. *Cancer* 109:2257–2267.
50. Brenner W, et al. (2002) Loss of tumor suppressor protein PTEN during renal carcinogenesis. *Int J Cancer* 99:53–57.
51. Giovannini M, et al. (2000) Conditional biallelic Nf2 mutation in the mouse promotes manifestations of human neurofibromatosis type 2. *Genes Dev* 14:1617–1630.
52. Kuhn R, Schwenk F, Aguet M, Rajewsky K (1995) Inducible gene targeting in mice. *Science* 269:1427–1429.
53. Mao X, Fujiwara Y, Orkin SH (1999) Improved reporter strain for monitoring Cre recombinase-mediated DNA excisions in mice. *Proc Natl Acad Sci USA* 96:5037–5042.
54. Taub M (2005) Primary kidney proximal tubule cells. *Methods Mol Biol* 290:231–247.
55. Chung SD, Alavi N, Livingston D, Hiller S, Taub M (1982) Characterization of primary rabbit kidney cultures that express proximal tubule functions in a hormonally defined medium. *J Cell Biol* 95:118–126.
56. Robine S, Jaisser F, Louvard D (1997) Epithelial cell growth and differentiation. IV. Controlled spatiotemporal expression of transgenes: New tools to study normal and pathological states. *Am J Physiol* 273(4 Pt 1):G759–762.
57. Maeshima A, Yamashita S, Nojima Y (2003) Identification of renal progenitor-like tubular cells that participate in the regeneration processes of the kidney. *J Am Soc Nephrol* 14:3138–3146.